UT Southwestern Medical Center

Department of Surgery

Axl is critical for pancreatic cancer cellular plasticity and metastasis

Wenting Du[1], Huocong Huang[1], Jason Toombs[1], Natalie Burton[1], Zhaoning Wang[2], Yuqing Zhang[1], Rolf A. Brekken[1]

[1]Department of Surgery and Hamon Center for Therapeutic Oncology Research, [2]Department of Molecular Biology, University of Texas Southwestern Medical Center, Dallas, TX

BACKGROUND

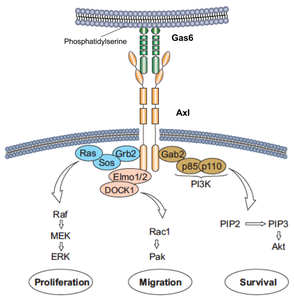

Modified from Pavel A. Levin, et al, *Journal of Thoracic Oncology*, 2016

Metastasis and resistance to chemotherapy remain the major challenges in the treatment of pancreatic ductal adenocarcinoma (PDAC) patients. Tumor-intrinsic and suppressive immune mechanisms contribute to chemotherapy failure. Strategies that enhance the efficacy of standard therapies are likely the most efficient route to improve overall survival in this disease.

Axl is a member of the TAM (Tyro3, Axl, MerTK) receptor tyrosine kinase family and participates in various cellular processes, including cell survival, proliferation, migration and epithelial plasticity. Growth arrest specific factor 6 (Gas6) is the ligand for Axl. Once Gas6 binds to Axl, it induces the dimerization of the Gas6/Axl binding complex. Ligand-induced activation of Axl occurs only after the Gla domain of Gas6 binds to phosphatidylserine. The Gas6-Axl pathway is estimated to be active in 70% of human pancreatic cancers where it correlates with an adverse clinical prognosis. Axl expression and activity are also associated with metastasis, therapy resistance, and immunosuppression in various types of cancers. Here we demonstrate the function of Axl in pancreatic cancer cellular plasticity and microenvironment, highlighting the importance of Axl on PDAC progression, metastases and chemoresistance.

I. Axl deficiency prolongs survival, inhibits metastasis and improves the sensitivity to gemcitabine in *KIC*

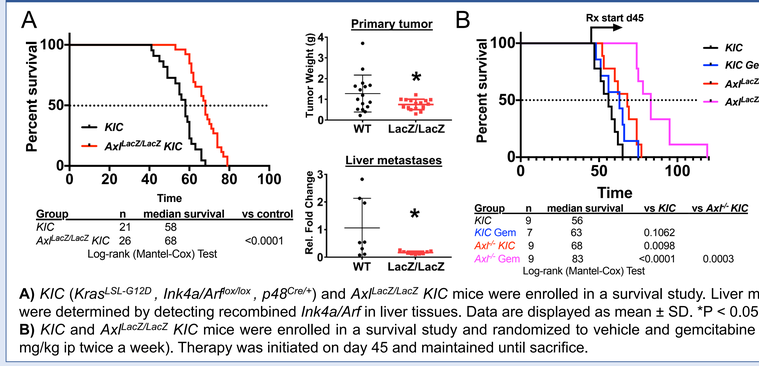

Group	n	median survival	vs control
KIC	21	58	
Axl$^{LacZ/LacZ}$ *KIC*	26	68	<0.0001

Log-rank (Mantel-Cox) Test

Group	n	median survival	vs *KIC*	vs *Axl*$^{-/-}$ *KIC*
KIC	9	56		
KIC Gem	7	63	0.1062	
Axl$^{-/-}$ *KIC*	9	68	0.0098	
Axl$^{-/-}$ Gem	9	83	<0.0001	0.0003

Log-rank (Mantel-Cox) Test

A) *KIC* (*Kras*$^{LSL-G12D}$, *Ink4a/Arf*$^{lox/lox}$, *p48*$^{Cre/+}$) and *Axl*$^{LacZ/LacZ}$ *KIC* mice were enrolled in a survival study. Liver metastases were determined by detecting recombined *Ink4a/Arf* in liver tissues. Data are displayed as mean ± SD. *P < 0.05; by t-test. **B)** *KIC* and *Axl*$^{LacZ/LacZ}$ *KIC* mice were enrolled in a survival study and randomized to vehicle and gemcitabine (Gem, 25 mg/kg ip twice a week). Therapy was initiated on day 45 and maintained until sacrifice.

II. *Axl-deficient KIC* displays a more differentiated histology and has a more inflammatory and active immune microenvironment

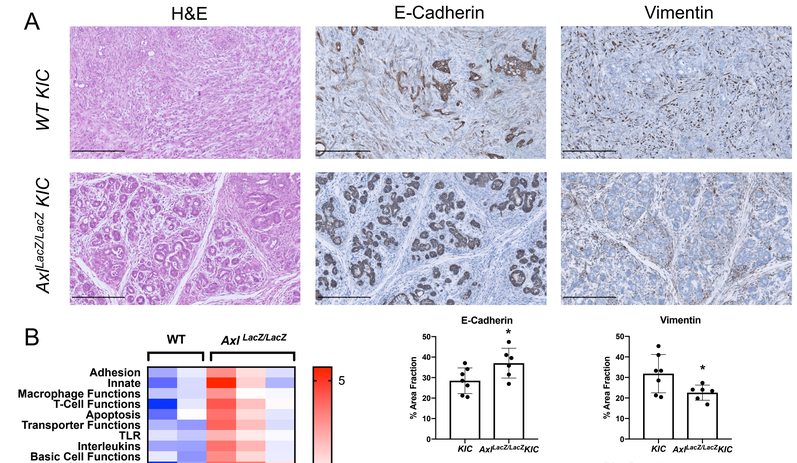

A) Tumor tissues from *KIC* and *Axl*$^{LacZ/LacZ}$ *KIC* mice were evaluated for indicated targets. Images were analyzed using ImageJ software; quantification of % area fraction is shown. Data are displayed as mean ± SD. *P < 0.05; by t-test. Scale bar, 250 μM. **B)** RNA was isolated from *KIC* and *Axl*$^{LacZ/LacZ}$ *KIC* tumors and was analyzed using Mouse PanCancer Immune Profiling Panel (NanoString Technologies). Upregulated (Red) and downregulated (Blue) gene programs/functions are shown.

III. Axl is highly expressed in mesenchymal PDAC tumor cells

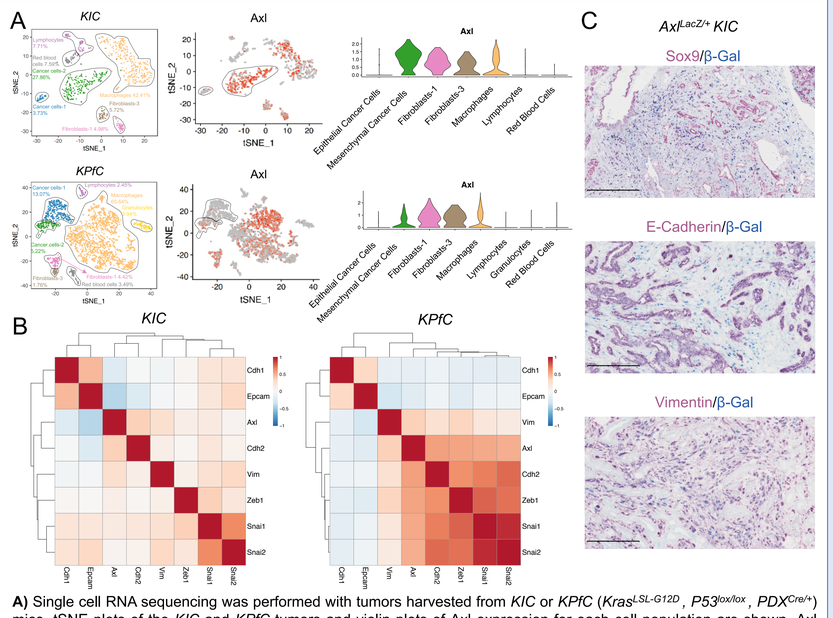

A) Single cell RNA sequencing was performed with tumors harvested from *KIC* or *KPfC* (*Kras*$^{LSL-G12D}$, *P53*$^{lox/lox}$, *PDX*$^{Cre/+}$) mice. tSNE plots of the *KIC* and *KPfC* tumors and violin plots of Axl expression for each cell population are shown. Axl expression is highlighted in red in the second tSNE plot for each mouse model. **B)** Correlation plots with Axl and EMT genes in *KIC* and *KPfC* models were generated by analyzing the EMT gene expression within the cancer cell clusters from each model. A positive correlation is highlighted in red and negative correlation is highlighted in blue. **C)** Tumor tissues from *Axl*$^{LacZ/+}$ *KIC* mice were evaluated for co-localization of β-galactosidase and tumor cell marker Sox9, epithelial marker E-Cadherin and mesenchymal marker vimentin. β-galactosidase staining is used to identify the expression of Axl.

IV. Axl expression on tumor cells is critical for PDAC progression and metastasis

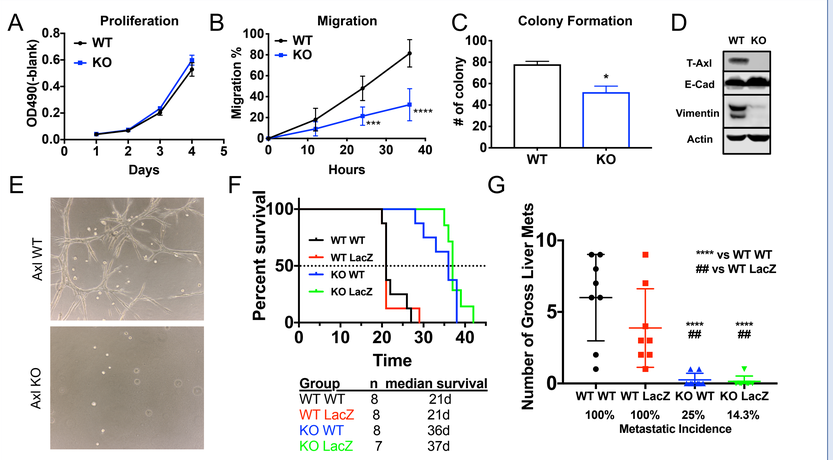

Group	n	median survival
WT WT	8	21d
WT LacZ	8	21d
KO WT	8	36d
KO LacZ	7	37d

A) Axl was ablated out using CRISPR-Cas9 in *KPfC* tumor cells. Cell proliferation was investigated in WT and Axl KO *KPfC* cells using MTS assay. **B)** Cell migration was investigated in WT and Axl KO *KPfC* cells by a "scratch" assay. Monolayers of the indicated cells were wounded with a pipet tip. The cells were incubated in 1% serum media. Wound closure was monitored at 12, 24, and 36 hours and is reported as % wound closure. ***P < 0.001; ****P < 0.0001; by t-test. **C)** Colony formation for WT and Axl KO *KPfC* cells is shown as mean + SD colonies/hpf . *P < 0.05; by t-test. **D)** Cell lysates from WT and Axl KO *KPfC* cells were evaluated for indicated targets by western blot. **E)** Representative pictures of WT and Axl KO *KPfC* cells grown in 30% matrigel+70% collagen for 4 days. **F)** WT and *Axl*$^{LacZ/LacZ}$ C57BL/6 orthotopically injected with WT and Axl KO *KPfC* cells were enrolled in a survival study. Groups were as follows: WT *KPfC* cells in WT C57BL/6 mice; WT *KPfC* cells in *Axl*$^{LacZ/LacZ}$ C57BL/6 mice; Axl KO *KPfC* cells in WT C57BL/6 mice; Axl KO *KPfC* cells in *Axl*$^{LacZ/LacZ}$ C57BL/6 mice. **G)** Number of gross liver metastases and metastatic incidence of the above survival study are shown. ****P < 0.0001 vs WT *KPfC* cells in WT C57BL/6 mice; ## P < 0.01 vs WT *KPfC* cells in *Axl*$^{LacZ/LacZ}$ C57BL/6 mice; by ANOVA.

V. Pharmacological inhibition of Axl reduces tumor progression and improves response to chemotherapy in vivo

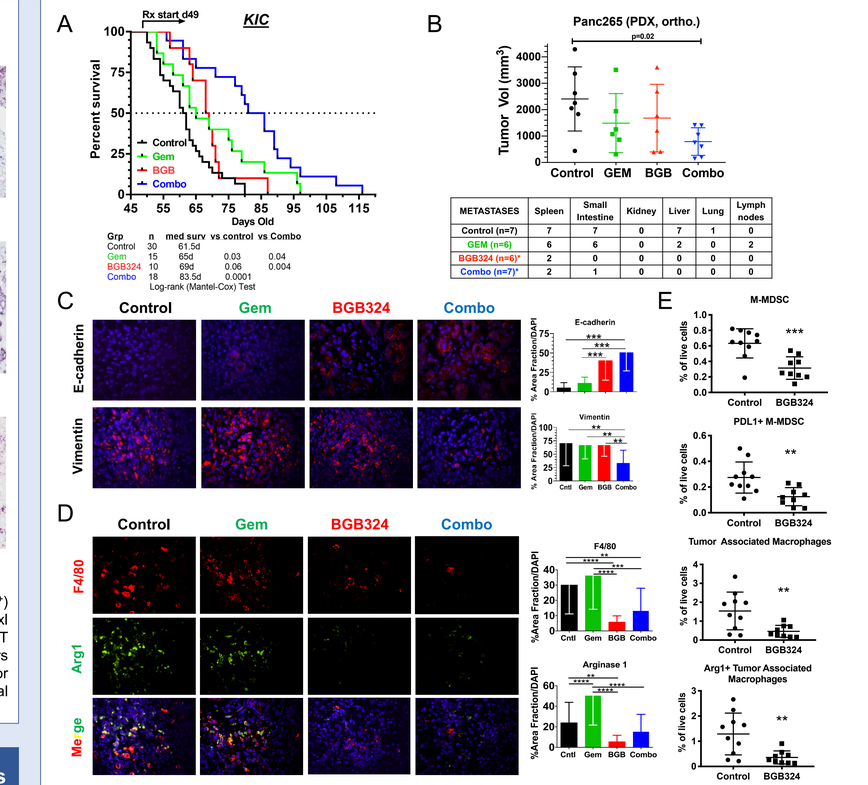

Grp	n	med surv	vs control	vs Combo
Control	30	61.5d		
Gem	15	65d	0.03	0.04
BGB324	10	69d	0.06	0.004
Combo	18	83.5d	0.0001	

Log-rank (Mantel-Cox) Test

METASTASES	Spleen	Small Intestine	Kidney	Liver	Lung	Lymph nodes
Control (n=7)	7	7	0	7	1	0
GEM (n=6)	6	6	0	2	0	2
BGB324 (n=6)*	2	0	0	0	0	0
Combo (n=7)*	2	1	0	0	0	0

Ludwig and Du, et al. *Cancer research*, 2018

A) *KIC* mice were enrolled in a survival study and randomized to vehicle (Control), BGB324 (50 mg/kg PO BID), gemcitabine (25 mg/kg ip twice a week), and gemcitabine + BGB324. Therapy was initiated on day 49 and maintained until sacrifice. **B)** Panc 265 was orthotopically implanted into nu/nu athymic mice. After tumor establishment, mice were treated as in **(A)** (n = 6-7/group). Total gross metastasis was determined by evaluation of liver, diaphragm, GI lymph nodes, and lung at the time of sacrifice. BGB324 alone or in combination with gemcitabine significantly reduced the rate of metastasis (p=0.001 vs control, Fisher's exact test). **C)** and **D)** Tumor tissues from *KIC* mice above were evaluated for indicated targets for epithelial (E-Cadherin) to mesenchymal (Vimentin) transition or immunosuppressive (Arginase 1) macrophages (F4/80). Images were analyzed using Elements software; quantification of % area fraction is shown. Data are displayed as mean ± SD and represent 5 images per tumor with 4 animals per group analyzed. **P < 0.01; ***P < 0.005; ****P < 0.001; by ANOVA. **E)** Flow cytometry of PDAC tumors treated with vehicle (Control) or BGB324 (50 mg/kg, PO, BID) for two weeks. BGB324 reduced monocytic MDSCs (M-MDSCs, CD11b+ Ly6G- Ly6C+), PD-L1+ M-MDSCs, tumor associated macrophages (CD11b+ Ly6G- Ly6C- F4/80+ CD11c+ MHCII+) and Arginase1+ tumor associated macrophages. **, P < 0.01; ***, P < 0.005 by t-test.

CONCLUSION

Pancreatic ductal adenocarcinoma, a leading cause of cancer-related death in the US, has a high metastatic rate that is associated with persistent immune suppression. Axl, a member of the TAM (Tyro3, Axl, MerTK) receptor tyrosine kinase family, has been identified as a critical factor that drives metastasis and immune suppression in many cancer types. Using genetically engineered mouse models, we demonstrate that:

- Axl-deficient PDAC bearing mice have longer median survival, smaller tumors, fewer metastases and higher sensitivity to chemotherapy (gemcitabine) compared to Axl WT PDAC mice.
- Axl-deficient PDAC displays a more differentiated histology and has a more inflammatory and active immune microenvironment.
- Axl is expressed highly in tumor cells that have a mesenchymal-like phenotype.

To study the contribution of Axl positive mesenchymal tumor cells, Axl was knocked out using CRISPR-Cas9 in primary tumor cells isolated from *KPfC* tumors. Characterizing these cells shows that:

- Axl-deficient PDAC cells displayed a more differentiated phenotype in vitro compared to Axl WT parental cells.
- Axl expression on tumor cells is critical for PDAC progression and metastasis.

As a potential therapeutic target, pharmacological inhibition of Axl by BGB324 significantly reduces tumor progression and metastasis and improves response to chemotherapy in multiple preclinical PDAC models. As a result, clinical testing of BGB324 (Bemcentinib) in conjunction with standard chemotherapies in pancreatic cancer patients has been initiated (NCT03649321) . Bemcentinib, as well as other strategies of Axl inhibition, is also being investigated as a single agent or in combination with targeted-, chemo-, and immunotherapy in different types of cancer patients.